PROCEEDINGS OF SCIENCE

Recent Results from the NA49 experiment

Christoph Blume for the NA49 Collaboration*
University of Frankfurt, Germany
E-mail: blume@ikf.uni-frankfurt.de

Recent results of the NA49 collaboration are presented. Transverse mass spectra as well as total multiplicities of identified particles are discussed. The study of their evolution from AGS over SPS to the highest RHIC energy reveals a couple of interesting features. These include a sudden change in the energy dependence of the m_t-spectra and of the yields of strange hadrons around 30*A* GeV. Additionally, new results on particle production at high-p_t for Pb+Pb collsions at 158*A* GeV, as well as on the v_2 of Λ, are discussed.

International Europhysics Conference on High Energy Physics
July 21st - 27th 2005
Lisboa, Portugal

*Speaker.

PoS(HEP2005)125

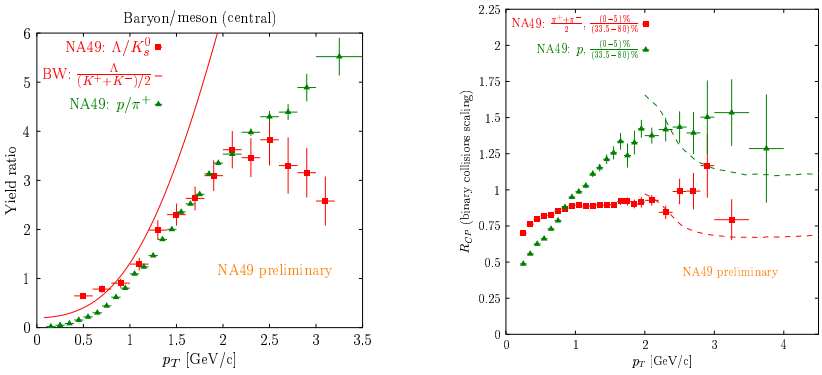

Figure 1: Left: The baryon/meson ratio as a funtion of p_t in central Pb+Pb reactions at $\sqrt{s_{NN}}$ = 17.2 GeV. The solid line represents the expectation from a fit with a Blast-Wave model [4]. Right: The nuclear modification factor R_{CP} as a function of p_t compared to a pQCD calculation including jet quenching (dashed lines).

1. Introduction

In the recent years the NA49 experiment has collected data on Pb+Pb collisions at beam energies between 20*A* and 158*A* GeV with the objective to cover the critical region of energy densities where the expected phase transition to a deconfined phase might occur in the early stage of the reactions. NA49 is a fixed target experiment at the CERN SPS. Details on the experimental setup can be found in [1].

2. High-p_t Spectra

Among the most interesting features discovered at RHIC is the suppression of high-p_t particle production in central nucleus-nucleus collisions relative to peripheral ones or p+p reactions. This suppression can be expressed by the ratio $R_{CP} = \frac{N_{coll}(per.)}{N_{coll}(cen.)} \frac{\text{Yield(cen.)}}{\text{Yield(per.)}}$. As shown in the right panel of Fig. 1, R_{CP} for charged pions always stays below unity for top SPS energies, even though a strong Cronin enhancement should be expected [2]. The data points for pions, as well as for kaons approach at higher p_t a pQCD prediction that includes jet quenching [3], indicating that this effect may already be present at top SPS energies.

The baryon/meson ratio clearly rises above unity for $p_t > 1.0$ GeV/c (see left panel of Fig. 1), similar as observed at the much higher RHIC energies. This might also point to a possible explanation in terms of quark coalescence models, as are discussed for higher energies.

3. Λ-Flow

Figure 2 shows the first results on elliptic flow of Λ from NA49. While the p_t-dependence is similar, the absolute values of v_2 for Λ are always below the ones for protons. This mass ordering is expected from hydrodynamic models, as illustrated by the blast wave fit [4]. The increase of v_2 with p_t is more pronounced at higher $\sqrt{s_{NN}}$ (see right hand side of Fig. 2), which is only partially due to the different centrality selection.

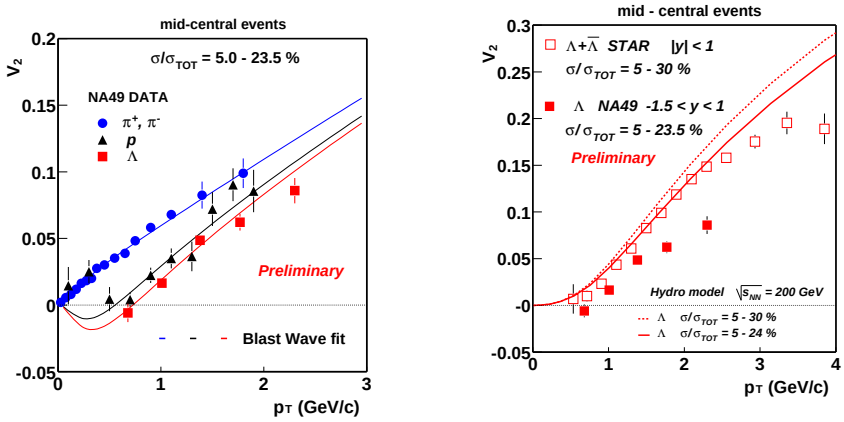

Figure 2: Left: The v_2 of charged pions, protons, and Λ as a function of p_t in semi-central Pb+Pb collisions at $\sqrt{s_{NN}}$ = 17.2 GeV. The solid lines represent results of a blast wave fit [4]. Right: The v_2 for Λ measured at $\sqrt{s_{NN}}$ = 17.2 GeV and $\sqrt{s_{NN}}$ = 200 GeV [5] in comparison to a hydrodynamical calculation [6].

4. Transverse mass spectra

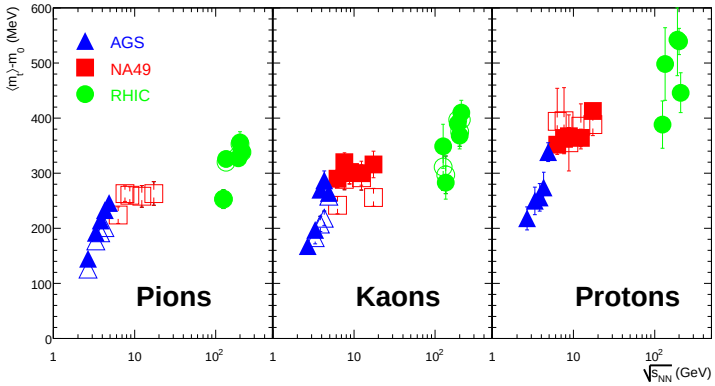

Figure 3: The energy dependence of $\langle m_t \rangle - m_0$ for pions, kaons, and protons at mid-rapidity for 5 (10%) most central Pb+Pb/Au+Au reactions. Open (solid) symbols represent negatively (positively) charged particles.

The increase with energy of the inverse slope parameter T of the kaon m_t-spectra, as derived from an exponential fit, exhibits a sharp change to a plateau around 30*A* GeV [7]. Since the kaon m_t-spectra – in contrast to the ones of the lighter pions or the heavier protons – have to a good approximation an exponential shape, the inverse slope parameter provides in this case a good characterization of the spectra. For other particle species, however, the local slope of the spectra depends on m_t. Instead, the first moment of the m_t-spectra can be used to study their energy dependence. The dependence of $\langle m_t \rangle - m_0$ on the center of mass energy $\sqrt{s_{NN}}$ is summarized in Fig. 3. The change of the energy dependence around a beam energy of 20 – 30*A* GeV is clearly visible for

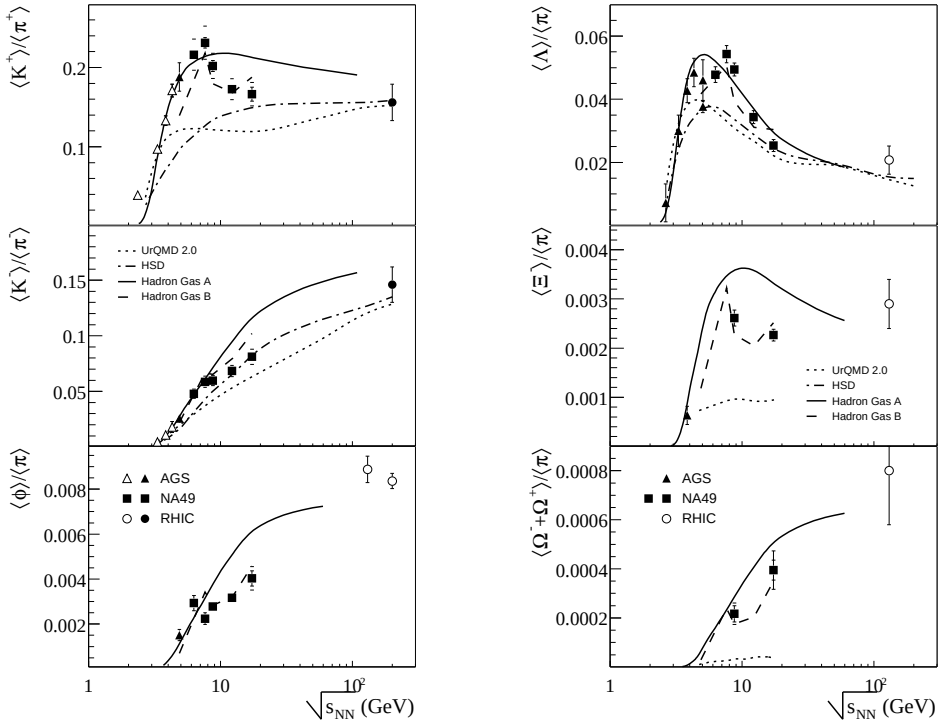

Figure 4: The energy dependence of the 4π-yields of strange hadrons, normalized to the pion yields, in central Pb+Pb/Au+Au collisions. The data are compared to string hadronic models [8, 9] (UrQMD 2.0: dotted lines, HSD: dashed-dotted lines) and statistical hadron gas models [10, 11] (with strangeness under-saturation: dashed line, assuming full equilibrium: solid line).

pions and kaons. While $\langle m_t \rangle - m_0$ rises steeply in the AGS energy range, the rise is much weaker from the low SPS energies on. To a lesser extent this change is also seen for protons.

5. Particle yields

In Fig. 4 the energy dependence of the total multiplicities for a variety of strange hadrons, normalized to the pion yield, is summarized and compared to model predictions. Generally, it can be stated that the string hadronic models UrQMD and HSD [8, 9] do not provide a good description of the data points. Especially the Ξ and Ω production is substantially underestimated and the maximum in the K^+/π^+ratio is not reproduced. The statistical hadron gas models [10, 11], on the other hand, provide a better overall description of the measurements. However, the introduction of an energy dependent strangeness under-saturation factor γ_S is needed [11], in order to capture the structures in the energy dependence of most particle species (K^+, K^-, ϕ, Ξ). This is seen in particular in the energy dependence of the total strangeness production (see Fig. 5), which changes around 30*A* GeV. The strangeness to pion ratio exhibits a pronounced maximum at this energy, which is not reproduced by the statistical hadron gas model [10], but may be related to the onset of deconfinement [13].

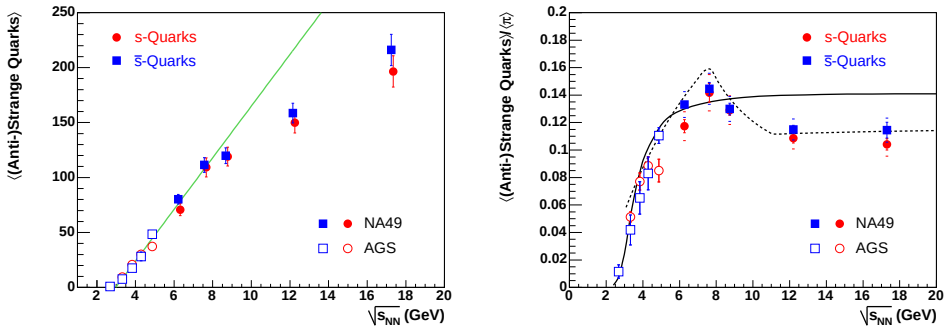

Figure 5: Left: The total number of strange quarks and anti-quarks as carried by kaons and hyperons versus the collision energy for central Pb+Pb (Au+Au) reactions (details see [12]). The line represents a linear fit to the low energy data. Right: The ratio of the number of strange quarks and anti-quarks to the pion yield as a function of $\sqrt{s_{\mathrm{NN}}}$. The solid line represents the statistical hadron gas model with full equilibration of strangeness [10], while the dashed line corresponds to the statistical model of the early stage [13].

References

[1] S.V. Afanasiev et al. (NA49 collaboration), Nucl. Instrum. Meth. **A 430** (1999), 210.

[2] A. Laszlo et al. (for the NA49 collaboration), arXiv:nucl-ex/0510054.

[3] X.N. Wang, Phys. Lett. **B 595** (2004), 165.

[4] F. Retiere and M.A. Lisa, Phys. Rev. **C 70** (2004), 044907.

[5] J. Adams et al. (STAR collaboration), Phys. Rev. Lett. **92** (2004), 052302.

[6] P. Huovinen, Nucl. Phys. **A 761** (2005), 296, and private communication.

[7] M. Gaździcki (for the NA49 collaboration), J. Phys. **G 30** (2004), S701.

[8] M. Bleicher et al., J. Phys. **G 25** (1999), 1859.

[9] E.L. Bratkovskaya et al., Phys. Rev. **C 69** (2004), 054907.

[10] P. Braun-Munziger, J. Cleymans, H. Oeschler, and K. Redlich, Nucl. Phys. **A 697** (2002), 902.

[11] F. Becattini, M. Gaździcki, A. Keränen, J. Manninen, and R. Stock, Phys. Rev. **C 69** (2004), 024905.

[12] C. Blume et al. (for the NA49 collaboration), J. Phys. **G 31** (2005), s685.

[13] M. Gaździcki and M.I. Gorenstein, Acta Phys. Polon. **B 30** (1999), 2705.